*Proc. Natl. Acad. Sci. USA*
Vol. 76, No. 7, pp. 3325–3329, July 1979
Biophysics

# Acoustic microscopy: Resolution of subcellular detail

**(ultrasound/mechanical properties/cytoplasmic thickness/nuclei, actin cables, and mitochondria)**

R. N. JOHNSTON*, A. ATALAR†, J. HEISERMAN†, V. JIPSON†, AND C. F. QUATE†‡

*Department of Biological Sciences, and †Edward L. Ginzton Laboratory, Stanford University, Stanford, California 94305

*Contributed by C. F. Quate, April 24, 1979*

**ABSTRACT** **Recent advances now permit the use of scanning acoustic microscopy for the analysis of subcellular components. By sequential viewing of identified fixed cells with acoustic, light, and electron microscopy, we have established that the acoustic microscope can readily detect such features as nuclei and nucleoli, mitochondria, and actin cables. Under optimal conditions, images can even be obtained of filopodia, slender projections of the cell surface that are approximately 0.1–0.2 μm in diameter. Small objects separated by as little as 0.5–0.7 μm can successfully be resolved. Three aspects of the acoustic micrographs prepared in this preliminary survey seem especially prominent. These are, first, the extraordinary level of acoustic contrast that can differentiate the various cytoplasmic organelles, even in regions of very thin cytoplasm; second, the reversals in acoustic contrast that occur when altering the plane of focus; and third, the sensitivity of the acoustic response to overall cytoplasmic thickness. The acoustic microscope uses a novel source of contrast that is based on local mechanical properties. In addition, it can provide a degree of resolution that is comparable to that of the light microscope.**

Much of our current understanding of cellular structure and function has been gained through the application of a variety of microscopic techniques. With light microscopy, advances in the methods of fixation and staining [for example, the recent development of immunofluorescence microscopy (see ref. 1)] and in optical systems [for example, phase contrast (2), Nomarski (3), Hoffman modulation (4), and polarized light microscopy (5)] have permitted major increases in knowledge about both living and fixed biological material. The electron microscope, in both the transmission and scanning modes, has of course greatly extended our understanding of the fine structure of nonliving preparations.

We now report the application of a novel type of microscopy, acoustic microscopy, to the analysis of subcellular components. We compare images obtained in the acoustic microscope with images of the same cells obtained by light and electron microscopy. This report is an update of an earlier paper (6), in which the visualization of single cells with the scanning acoustic microscope was first described. Since then, advances in acoustic technology have permitted major increases in resolution to a level now comparable to that of light microscopy (7). The impetus toward development of the acoustic microscope rests on the unique method of analysis, the use of high-frequency sound waves. The properties detected by acoustic radiation are different from those detected by either light or electron radiation, and present exciting possibilities for the examination, in a fundamentally new way, of biological material.

The publication costs of this article were defrayed in part by page charge payment. This article must therefore be hereby marked "*advertisement*" in accordance with 18 U. S. C. §1734 solely to indicate this fact.

## THE ACOUSTIC MICROSCOPE

The scanning acoustic microscope used in this study was introduced in 1974 by Lemons and Quate (8). The basic functioning of the device as used in the reflection mode can be understood with the aid of Fig. 1. An acoustic transducer mounted on the back of a sapphire rod is excited by applying an electric pulse at radio frequencies. This generates a collimated acoustic beam which propagates down the sapphire rod. At the front face of the rod a spherical depression in contact with a coupling fluid—in this case, water—forms an acoustic lens, and the acoustic beam is focused in the water according to Snell's law. In fact, due to the large difference in the velocity of sound between sapphire and water (a factor of 7.4), the focused beam suffers negligible spherical aberration and converges to a diffraction-limited spot (9). The object to be examined is placed at or near the focus. It is mechanically scanned line by line in a raster pattern. Acoustic power reflected by the object is collected and recollimated by the lens and detected (in a phase-sensitive way) by the transducer. The mechanical motion of the object is synchronized with a cathode ray display monitor and the variations in reflected acoustic power are used to modulate the intensity of the display. The image thus formed on the monitor screen can then be recorded photographically.

Resolution is determined by the diameter of the focal spot, which is, in turn, determined by the wavelength of the acoustic radiation in the water. Increasing the operating frequency of the instrument improves resolution by decreasing the acoustic wavelength. The maximum operating frequency is limited, however, because attenuation of the acoustic beam by the water increases as the square of the frequency. Using water at a temperature of 40–50°C and a lens focal length of 40 μm, the acoustic microscope is presently limited to operating frequencies of 2.6 GHz and hence to a wavelength in water of 0.6 μm. Greater resolution can be obtained by heating the water to a higher temperature (because the acoustic attenuation in water decreases with increasing temperature), by using a lens of smaller focal length, or by using a liquid of lower acoustic attenuation than water (D. Rugar, J. Heiserman, and C. F. Quate, unpublished data).

The variations in intensity of the reflected sound that lead to contrast in the acoustic image can arise in a number of ways. When the object is irregular on a scale that is either considerably greater than or comparable to the acoustic wavelength in water, then specular or diffuse scattering of sound occurs, respectively. When the object to be studied has acoustic properties similar to water (as is usually the case with biological materials), then sound enters the object and will be partially absorbed and phase shifted because of the viscosity or stiffness of the object. For solid objects (such as the glass slides on which biological samples are

‡ To whom requests for reprints should be addressed.

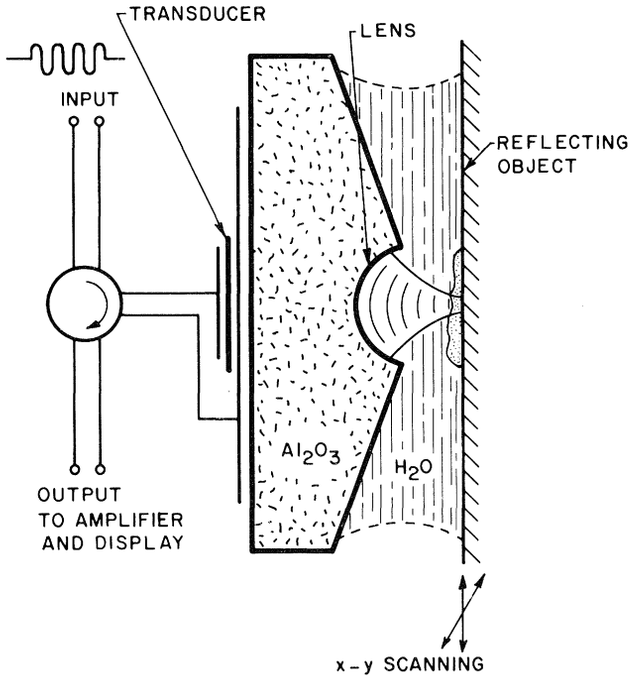


FIG. 1. Schematic illustration of the scanning acoustic microscope. See text for details of operation.

frequently mounted for observation), most of the sound is reflected but, depending on the position of focus, phase shifts may be introduced in the process of reflection. These events can all lead to variations in contrast of images of biological samples (10).

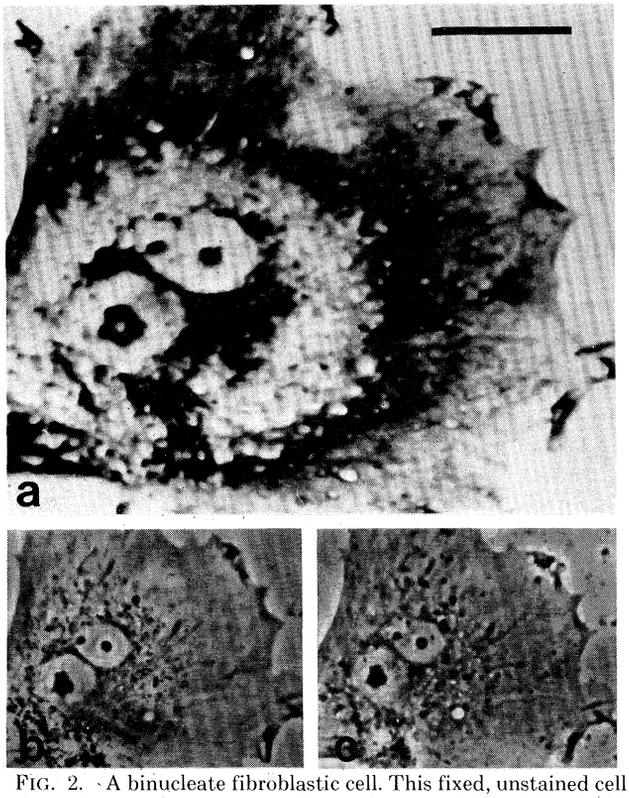


FIG. 2. A binucleate fibroblastic cell. This fixed, unstained cell was photographed with phase-contrast light microscopy before (*b*) and after (*c*) use of the acoustic microscope; gross damage to the cell does not occur as a result of acoustic microscopy. In the acoustic image (*a*), the nuclei and nucleoli exhibit great contrast with respect to the surrounding cytoplasm. Also note the ruffles of the cell periphery, the apparent granularity of the cell cytoplasm, and the alternating concentric bands of acoustic density. Bar indicates 10 $\mu$m.

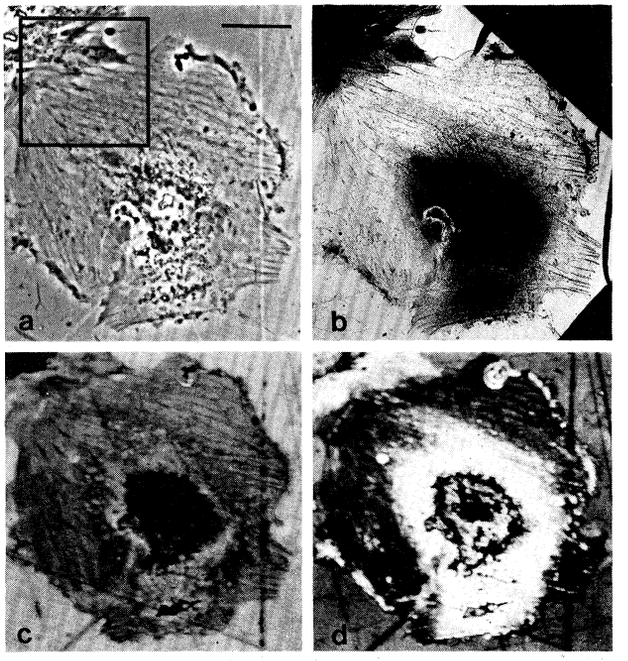


FIG. 3. Comparison of light, electron, and acoustic micrographs. This cluster of cells was photographed with phase-contrast (*a*) and transmission electron (*b*) microscopy after preparation of the acoustic micrographs (*c* and *d*). (These cells were also photographed by Nomarski and polarized light microscopy but, for the sake of brevity, these images are not included.) The two acoustic images were prepared at slightly different planes of focus. The large dark areas of *b* represent bars of the copper grid. The region outlined in *a* is shown at higher magnification in Fig. 4. Bar indicates 30 $\mu$m.

## MATERIALS AND METHODS

**Cell Culture.** Ciliary ganglia of embryonic chickens (8–9 days of incubation) were dissociated into suspensions of single cells with 0.1% trypsin (Microbiological Associates, Bethesda, MD) (11). These cells were then incubated in a humidified 5% $CO_2$ atmosphere at 37°C, in medium F-12 (GIBCO) supplemented with 10% fetal bovine serum (Microbiological Associates), for 2–5 days. The cells were grown at a density of 2–5 $\times 10^3$ cells per $cm^2$ either on collagen-coated glass discs (18 mm diameter) or on discs first covered with a film of Formvar (12), then coated with collagen. The reusable glass discs were designed both to fit the specimen holder of the acoustic microscope and to permit observation of identified cells in the light microscope and (when used with Formvar) in the transmission electron microscope.

**Preparation for Microscopy.** In all cases, samples were fixed with 2.5% glutaraldehyde in Sorenson's buffer (0.97% salts/0.12 M sucrose, 37°C, 20 min), then rinsed thoroughly with buffer. When samples were compared by only acoustic and light microscopy, cells of interest were first identified by the light microscope [Zeiss Photomicroscope; 40× (numerical aperture of 0.75) and 100× (oil-immersion, numerical aperture of 1.30) objectives]. They were then examined acoustically in distilled water, and later reexamined with the light microscope, with photographs prepared at each stage. Samples were examined in distilled water to avoid the crystallization of salts that would otherwise occur because of evaporation from the open-air specimen mount. (Newer microscopic designs will soon permit the examination of cells in media with salts.) Samples viewed

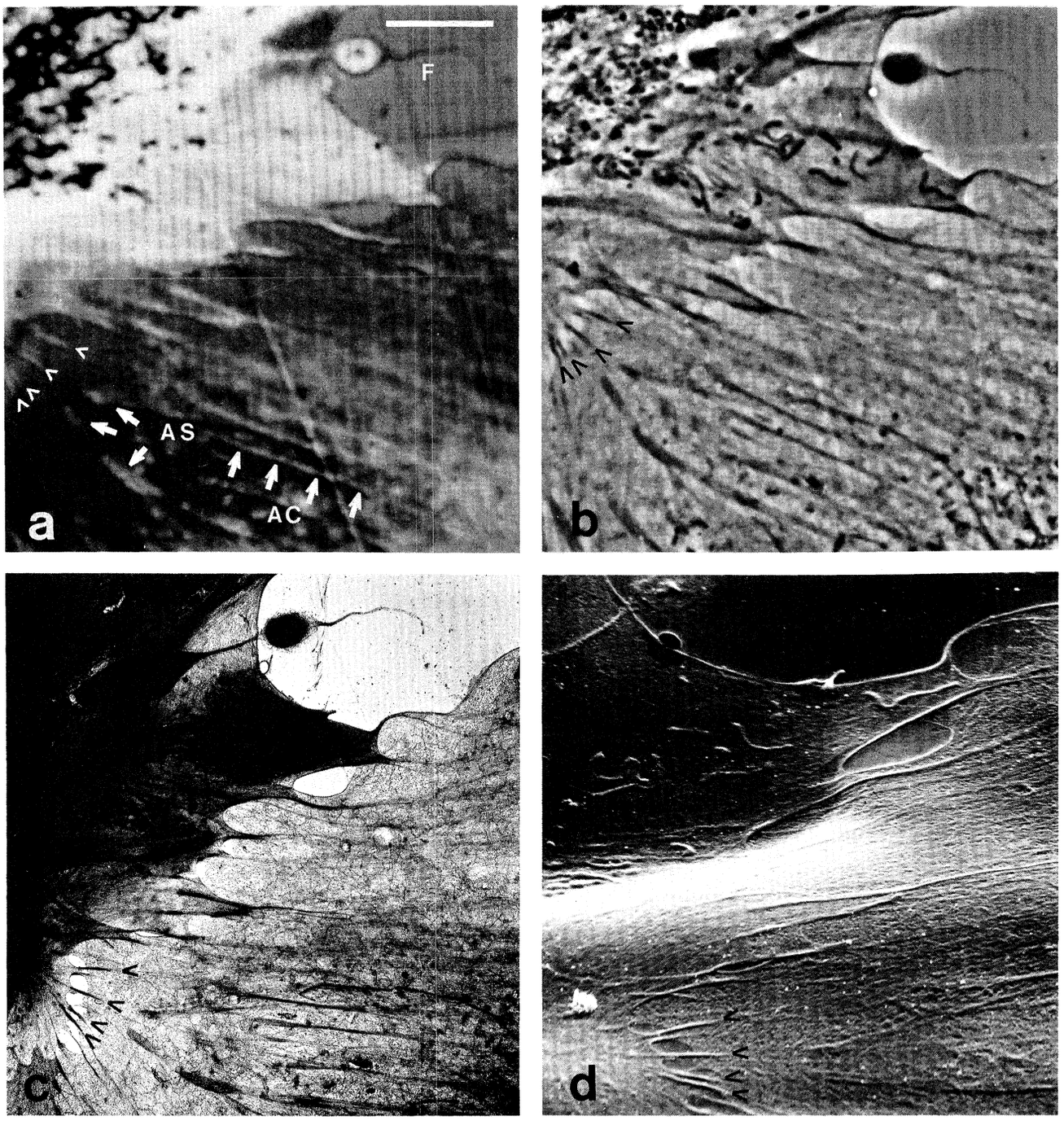


FIG. 4. Region of cellular interaction. This region is shown at a lower magnification in Fig. 3*a*. The acoustic micrograph (*a*) represents the greatest practical magnification now available with the acoustic microscope. The filopodium (F) and the sites of cell–cell attachment (arrowheads) are approximately 0.2 $\mu$m in diameter; the attachment sites are separated by as little as 0.5 $\mu$m. Actin cables (AC) and the oval expansions of their tips that may represent sites of cell–substratum attachment (AS) are clearly visible in the acoustic micrograph. These structures can also be seen in the phase-contrast (*b*) and the transmission electron (*c*) micrograph. Some of these structures are also visible in the scanning electron micrograph (*d*) as variations in surface contour; the broad undulations of the cells in *d* are caused by folding of the Formvar. Bar indicates 10 $\mu$m.

with acoustic, light, and electron microscopy were fixed with glutaraldehyde, as before, then rinsed, post-fixed with 0.2% $OsO_4$ (20°C, 10 min), rinsed again, lightly stained with uranyl acetate and lead citrate (13), and stored in buffer until use. After examination of selected cells with light and acoustic microscopy, small fragments of the Formvar plastic (with the adherent cells) were peeled off the glass disc, attached to copper grids (12), and dried at the critical point of $CO_2$. Up to the time of critical point drying, care was taken to keep the samples continually wet. Nevertheless, because the acoustic specimen holder was open to the atmosphere, it is possible that some preparations dried transiently in air. After the cells were photographed with the transmission electron microscope (Hitachi HU-11E-1, operated at 75 kV accelerating voltage), they were sputter-coated with gold (Denton Vacuum DV-502) and examined in the scanning electron microscope (Coates and Welter, model 50).

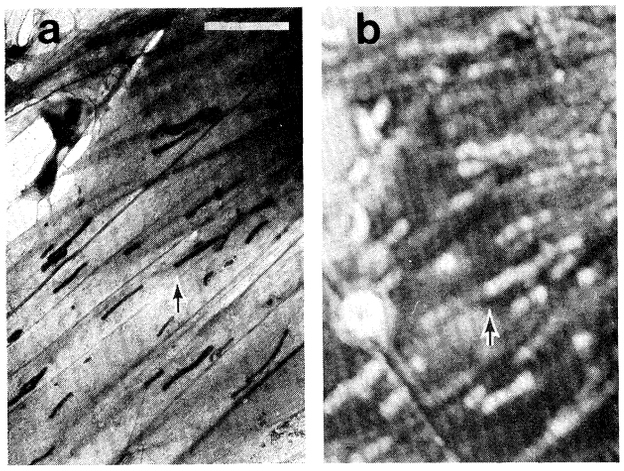


FIG. 5. Transmission electron (*a*) and acoustic (*b*) micrographs of a cluster of large mitochondria (arrow) aligned parallel to actin cables. Bar indicates 10 $\mu$m.

## RESULTS

Even in early experiments of this series, we were able to obtain dramatic acoustic images of fixed, unstained fibroblastic cells (Fig. 2*a*). Several prominent characteristics of acoustic images distinguish them from phase-contrast light micrographs of the same cells (Fig. 2 *b* and *c*). These characteristics include the roughly concentric dark and light bands that alternate inward from the edge of the cell. Superimposed upon these bands are the local dramatic variations in acoustic response that indicate the various cytoplasmic organelles. Initially, we were concerned that cellular structure might be damaged in some way by the high frequency sound waves used in acoustic microscopy (perhaps because of local heating by the acoustic beam) or by warming of the fluid in which the cells were bathed. Nevertheless, light micrographs prepared of cells before (Fig. 2*b*) and after (Fig. 2*c*) acoustic microscopy reveal that, at this level, cellular damage caused by the acoustic microscope is not great, consistent with the finding that acoustic microscopy is compatible with living cells (6).

In order to identify unambiguously the cytoplasmic organelles visible with acoustic microscopy and to evaluate possible mechanisms of formation of the concentric acoustic rings, we undertook a series of experiments designed to permit examination of identified cells by electron, light, and acoustic microscopy. Although it was technically difficult to identify and view single cells by these different approaches, we were nevertheless able, in a few cases, to examine cells with all these

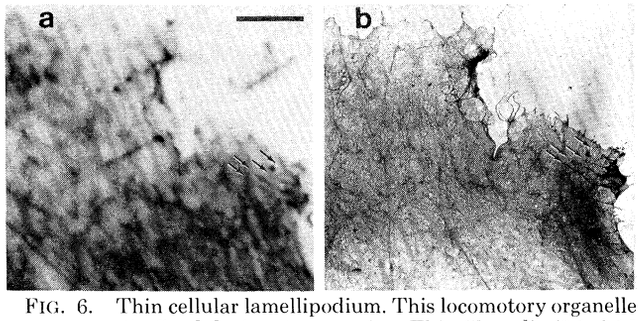


FIG. 6. Thin cellular lamellipodium. This locomotory organelle was apparently fixed during its extension. Thin filopodia (0.1–0.15 $\mu$m in diameter) protrude from the lamellipodium, and some of these (arrows) are faintly visible in the acoustic micrograph (*a*). Also note the irregular cytoplasmic lattice in *a* that is visible in the electron micrograph (*b*) as localized aggregations of microfilaments. Bar indicates 10 $\mu$m.

methods. To facilitate the penetration of electrons through whole-mounted cells in the transmission electron microscope, we selected for viewing those cells that appeared thin in the light microscope. An example of such a cell is illustrated in Fig. 3. The marked changes in patterns of acoustic contrast that result from a slight shift in positioning of the cell along the acoustic axis of the lens are demonstrated in Fig. 3 *c* and *d*. Although the concentric nature of the bands is essentially retained, their radial position, and the acoustic signal from the surrounding substratum, both vary with the separation between sample and lens and, thus, with the phase angle of the reflected acoustic signal. At this low magnification, relatively little cytoplasmic detail is revealed in the acoustic micrographs. Although more detail is visible in the light micrograph, contrast is reduced relative to the acoustic image. The corresponding electron micrograph shows great contrast and resolution, especially at the cell periphery, but penetration of the electron beam through the thicker central cytoplasm is too poor to reveal cellular detail.

In Fig. 4, the area outlined in Fig. 3*a* is shown at the highest magnification now practical with the acoustic microscope. Here, the detail revealed in the acoustic image closely approaches that obtained with a light microscope fitted with a 100× oil-immersion objective. Using the transmission electron micrograph as a reference, we are able to identify many of the acoustically visible structures, including an elongate filopodium, sites of attachment between adjacent cells, actin cables, and probable sites of cell–substratum attachment. Independent calibrations of these light and electron micrographs reveal that the indicated sites of cell–cell attachment, and the filopodium, are 0.2 $\mu$m in diameter. The scanning electron micrograph of the same region demonstrates that at least some of these features are visible as variations in surface contour, especially in regions where the cytoplasm is particularly thin. This variation in surface contour was unexpected, and may be artifactual. Note also that the cell thickness increases centrally.

Fig. 5 illustrates a portion of a cell that had an unusually prominent accumulation of mitochondria aligned parallel to a series of actin cables. The mitochondria present an acoustic image that contrasts dramatically with that of the surrounding cytoplasm. Whereas large mitochondria appear distinct, smaller mitochondria nearby are only poorly resolved acoustically, and their images are reduced in contrast.

The smallest biological objects we have yet been able to identify in the acoustic microscope are shown in Fig. 6. Here, an exceedingly thin portion of cell cytoplasm was apparently fixed during its extension as a ruffling membrane. Several filopodia, 0.1–0.15 $\mu$m in width, project from this membrane (Fig. 6*b*), and some of these are faintly visible in the acoustic image (Fig. 6*a*). Also visible acoustically is a diffuse and irregular cytoplasmic lattice, which corresponds in the electron micrograph to local aggregations of microfilaments.

## DISCUSSION

This study represents a successful attempt to specifically observe intracellular structure with the acoustic microscope. For this work, we selected fibroblastic cells of the peripheral nervous system, both because these cells were readily accessible to us and because their structure has previously been well characterized (14). By making comparisons among sequential acoustic, electron, and light micrographs of single cells, we have been able to identify acoustically prominent organelles that correspond to nuclei and nucleoli, mitochondria, actin cables and presumptive cell attachment sites, and filopodia, ruffles, and other cell surface projections.

The smallest biological objects that we are presently able to

detect acoustically, such as filopodia and other thin organelles, have diameters of 0.1–0.2 $\mu$m, though these are identifiable only when other organelles are not nearby. The ability of the acoustic microscope to resolve adjacent small objects is somewhat less. We estimate that the minimal separation of biological objects that can be acoustically resolved is about 0.5–0.7 $\mu$m, or approximately one wavelength. Although a light microscope equipped with an oil-immersion lens can surpass this performance, the difference is not great. We anticipate that improvements in acoustic microscopy over the next few years will narrow this gap further, and the acoustic instrument may in time even exceed the resolving power of the light microscope. Electron microscopists, of course, need not fear competition on this front.

Nevertheless, the acoustic microscope already offers potentially useful features that are characteristic of neither light nor electron microscopy. First, the degree of acoustic contrast that differentiates cytoplasmic organelles can be impressive, even when these organelles are unstained. Second, the acoustic microscope is apparently sensitive to slight variations in cytoplasmic thickness and provides a degree of information that is otherwise readily obtainable only in the interference microscope or in the scanning electron microscope. Finally, the acoustic microscope, unlike the electron microscope, is compatible with living cells (6).

The precise mechanisms by which biological objects generate acoustic contrast are not yet well understood. Localized changes in cytoplasmic mechanical properties, which could result in variations both in acoustic absorbance and in phase angle of the reflected signal, should contribute to acoustic contrast (15, 16). The phase angle of the acoustic response can vary as a function of at least two cytoplasmic parameters. An acoustic pulse propagating through a region of reduced density or increased mechanical stiffness would increase in velocity of propagation and thereby undergo a phase advance with respect to adjacent signals. Depending on the plane of acoustic focus, this would be interpreted by the microscope as either a relative lightening or a relative darkening of the visual image. On the other hand, an acoustic pulse propagating through a homogeneous object that is of variable thickness would undergo a greater phase advance, perhaps through multiples of $\pi$, in the thicker regions. We suspect that the latter mechanism may account, in large part, for the existence of the acoustic rings that appear to follow the contours of cells as they thicken toward their centers. We do not yet know, however, to what extent the local variations in acoustic contrast that are associated with cytoplasmic organelles correlate with mechanical or viscoelastic properties that might result in acoustic absorbance or phase shift. To answer these and other questions, further comparisons among acoustic and electron microscopic images of cells must be made.

We thank Kate Barald, Paul Green, and Norman Wessells for criticisms of this manuscript. We also thank Belen Palmer and Fran Thomas for technical assistance. The culturing of cells and light and electron microscopy were performed in Wessells' laboratory. This work was supported by Research Grants 1 R01 GM-25826-01 and RG HD-04708 from the National Institutes of Health. R.N.J. was partially supported by a Natural Sciences and Engineering Research Council of Canada scholarship.

1. Osborn, M. & Weber, K. (1977) *Cell* **12,** 561–571.
2. Zernike, F. (1942) *Physica* **9,** 686–974.
3. Allen, R. D., David, G. B. & Nomarski, G. (1969) Z. *Wissenschaft. Mikrosk. und Mikrosk. Tech.* **69,** 193–221.
4. Hoffman, R. (1977) *J. Microsc.* **110,** 205–222.
5. Inoué, S. (1952) *Exp. Cell Res. Suppl.* **2,** 305–318.
6. Lemons, R. A. & Quate, C. F. (1975) *Science* **188,** 905–911.
7. Jipson, V. & Quate, C. F. (1978) *Appl. Phys. Lett.* **32,** 789–791.
8. Lemons, R. A. & Quate, C. F. (1974) *Appl. Phys. Lett.* **24,** 163–165.
9. Lemons, R. A. & Quate, C. F. (1973) in *Proceedings of the Ultrasonics Symposium,* ed. deKlerk, J. (IEEE, New York), pp. 18–20.
10. Atalar, A. (1978) *J. Appl. Phys.* **49,** 5130–5139.
11. Helfand, S. L., Smith, G. A. & Wessells, N. K. (1976) *Dev. Biol.* **50,** 541–547.
12. Buckley, I. K. & Porter, K. R. (1975) *J. Microsc.* **104,** 107–120.
13. Ludueña, M. A. & Wessells, N. K. (1973) *Dev. Biol.* **30,** 427–440.
14. Wessells, N. K., Ludueña, M. A., Letourneau, P. C., Wrenn, J. T. & Spooner, B. S. (1974) *Tissue Cell* **4,** 757–776.
15. Atalar, A., Jipson, V., Koch, R. & Quate, C. F. (1979) *Annu. Rev. Mater. Sci.* **9,** 255–281.
16. Marmor, M. F., Wickramasinghe, H. K. & Lemons, R. A. (1977) *Invest. Ophthalmol. Vis. Sci.* **16,** 660–666.